JOURNAL OF THERMOPHYSICS AND HEAT TRANSFER
Vol. 15, No. 1, January–March 2001

Oxygen Atoms' Effect on Vibrational Relaxation of Nitrogen in Blunt-Body Flows

Eswar Josyula*
U.S. Air Force Research Laboratory, Wright–Patterson Air Force Base, Ohio 45433-7913

Numerical simulations are presented of the steady-state airflow over a hemisphere cylinder of 1-m radius having hypersonic Mach numbers, where vibrational relaxation is the dominant mechanism and the dissociation of oxygen is small. A Mach 6.5 flow was analyzed at freestream pressure of 50 Pa with a nonequilibrium freestream translational temperature of 300 K and vibrational temperature of 4000 K; a Mach 1.5 flow was also studied to delineate effects of vibration–translation (V–T) energy losses due to N_2–O collisions. The effects on the vibrational population distribution, temperature, and pressure in the flowfield were studied for various media: pure nitrogen and air mixtures of 0.0001, 0.1, and 1% oxygen atoms. Code validation was performed with previously reported computational results and experimental data for equilibrium flow in freestream, but nonequilibrium in the shock layer. An upwind difference numerical scheme was used to solve the inviscid Euler equations coupled to a vibrational kinetics model of N_2, assumed as an anharmonic oscillator of 40 quantum levels. The shock-standoff distance comparison with experimental data for a Mach 7.7 and 8.6 airflow past a blunt body showed good agreement. For the Mach 1.5 flow at nonequilibrium freestream conditions, the high efficiency of the V–T rates of N_2–O collisions introduces additional heating in the shock layer for 0.1% and higher atomic oxygen, thus increasing the shock-standoff distance; for the Mach 6.5 flow, a 0.1% atomic oxygen in air decreases the translational temperature in air compared to that of pure nitrogen in the stagnation region.

Nomenclature

e	=	total energy per unit mass
i, j	=	species indices in quantum levels v and w
M	=	Mach number; molecular weight
p	=	pressure
r	=	nose radius
T	=	translational temperature
T_{v1}	=	first-level vibrational temperature
Tv	=	vibrational temperature for which population densities correspond to a Boltzmann distribution
$\boldsymbol{u}$	=	velocity vector
v, w	=	vibrational quantum numbers
x, y	=	Cartesian coordinates
$\bar{\bar{\delta}}$	=	Kronecker delta function
Θ_v	=	characteristic temperature of vibration
θ	=	angular spacing, deg
ρ	=	mixture density
ρ_s	=	density of species, s
ρ_v	=	state density in the vth vibrational level
∞	=	freestream conditions index

Introduction

THE presence of a strong bow shock wave in hypersonic flow past a blunt forebody presents considerable difficulties for accurate numerical simulation of the flowfield in the stagnation region. The shock wave converts the high kinetic energy of the oncoming flow into various internal energy modes, which relax slowly and lead to significant chemical and thermal nonequilibrium in the stagnation region. Molecular collisions in a gas change the translational, rotational, vibrational, and electronic energies of the collision partners. The probabilities or effective cross sections of these elementary processes differ significantly, which give rise to widely separate relaxation times for the internal modes. Thus, it becomes important to account for the rates of relaxation processes to predict the nonequilibrium behavior of these kinds of flows. Vibrational equilibration is a process with relaxation times between the very short times for translational/rotational equilibration and the longer times for chemical and ionization equilibration. Vibrational energy distributions during relaxation are required for prediction of dissociation rates, interpretation of radiation experiments, and interpretation of ionic recombination rates that depend also on the electron energy distribution.[1] The instability of shock waves in gases and the anomalous relaxation in nonequilibrium states enhancing the perturbations of the gasdynamic quantities were discussed in Ref. 2.

Studies were conducted in the 1960s showing the high efficiency with which the vibrational relaxation of molecular species takes place in the presence of minor amounts of oxygen atoms.[3,4] These experiments indicate that oxygen atoms are several orders of magnitude more efficient than O_2 or N_2 in the vibrational relaxation of O_2 and N_2, respectively. This highly efficient relaxation is attributed to a chemical effect resulting from strong attractive intermolecular forces.[4] It is well known that the vibrational relaxation time for O_2 is, at a given temperature, smaller than that for N_2 because the natural frequency in N_2 is one and one-half times higher than oxygen. This makes the excitation of vibrational modes in nitrogen more difficult, which results in first oxygen and then nitrogen reaching equilibrium.[5] Also, O_2–O_2 collisions are 2.5 times more effective than N_2–N_2 collisions. However, in air, a considerable degree of N_2 relaxation is achieved by the presence of oxygen atoms. Breshears and Bird[3] report that the experimental values obtained for the vibrational relaxation time for nitrogen dilute in 1 atm of oxygen atoms are nearly two orders of magnitude below the values of pure nitrogen. Study of N_2–O collisional effects on the vibrational relaxation of N_2 in high-speed airflow past a blunt body is one of the objectives of the present paper.

Earlier work of Josyula[6] showed thermal nonequilibrium effects due to a higher vibrational temperature than the translational temperature behind the shock wave for a Mach 6.5 flow of pure nitrogen past a blunt body. The additional energy contained initially in the vibrational modes is cooled in the shock layer exhibiting greater non-Boltzmann distributions due to nonresonant energy exchanges and higher populations in the upper levels. This resulted in an increase in shock-standoff distance compared to the flow having equilibrium freestream conditions. The present study includes the various components of air with varying amounts of atomic oxygen concentration

Received 29 November 1999; revision received 10 July 2000; accepted for publication 18 July 2000.

*Research Aerospace Engineer, Air Vehicles Directorate. Associate Fellow AIAA.

for flow past a blunt body, the shock layer undergoing vibrational cooling.[6] To isolate the effects of the vibrational–translational (V–T) energy losses in the flowfield, a Mach 1.5 flow of air was studied for its low translational temperature; atomic oxygen at these low temperatures being negligibly small, higher concentrations were introduced in the flowfield to increase the probability of N_2–O collisions and to determine a rate controlling atomic oxygen mass fraction for V–T heating. A similar study was conducted by Candler and Kelley[7] using a harmonic oscillator assumption for the molecules, where the effect of upstream vibrational energy excitation on a supersonic airflow increased the shock-standoff distance and resulted in a reduction in drag for a Mach 1.3 airflow past a 1-cm-radius sphere.

The composition of air at a temperature below 3000 K is such that the nitrogen dissociation does not start and oxygen dissociation just begins to form a mixture composition that has minor amounts of oxygen atoms. The effect of these minor amounts of oxygen atoms on the vibrational relaxation of N_2 behind the blunt-body shock wave, and the subsequent effect on the shock wave, is the objective of the present study. The paper describes a study in which the vibrational relaxation of nitrogen in the presence of oxygen atoms was computed for shock temperatures of 450 and 3000 K. The study consists of flow past blunt body of 1-m radius at freestream Mach numbers of 1.5 and 6.5 at a translational temperature of 300 K and vibrational temperature of 4000 K and freestream pressure of 50 Pa. Because of the large disparity of vibrational relaxation times of pure nitrogen and nitrogen in the presence of oxygen atoms, the results using both flow media (that of pure nitrogen and air mixtures) are compared to assess the effect of N_2–O collisions on N_2 relaxation. The nitrogen molecule is treated as anharmonic oscillator with 40 quantum energy levels for performing a detailed study of the nonequilibrium phenomenon in the slower relaxing nitrogen. The oxygen molecule is assumed as a harmonic oscillator with V–T energy transfers evaluated using the Landau–Teller theory. In the present study, the species, N_2, O_2, and O were considered to make up the air mixture. Code validation consists of comparisons of temperature profiles with previously reported computations and shock-standoff distances with previously reported experimental data of flows at intermediate hypersonic Mach numbers.

Analysis

The global conservation equations in mass-averaged velocity form are

$$\frac{\partial}{\partial t}(\rho_v) + \nabla \cdot (\rho_v \boldsymbol{u}) = \dot{\omega}_v \qquad v = 0, 1, \ldots \tag{1}$$

$$\frac{\partial}{\partial t}(\rho_s) + \nabla \cdot (\rho_s \boldsymbol{u}) = \dot{\omega}_s \tag{2}$$

$$\frac{\partial}{\partial t}(\rho \boldsymbol{u}) + \nabla \cdot (\rho \boldsymbol{u}\boldsymbol{u} - p\bar{\bar{\delta}}) = 0 \tag{3}$$

$$\frac{\partial}{\partial t}(\rho_s e_{\text{vib}}) + \nabla \cdot (\rho_s e_{\text{vib}} \boldsymbol{u}) = \rho_s \dot{\omega}_{\text{vib}} \tag{4}$$

$$\frac{\partial}{\partial t}(\rho e) + \nabla \cdot \left[\rho\left(e + \frac{p}{\rho}\right)\boldsymbol{u}\right] = 0 \tag{5}$$

The conservation equation (1) is written for mass density in quantum level v for diatomic nitrogen. The source term $\dot{\omega}_v$ derived from the vibrational master equations is made up of the relevant energy exchange processes consisting of the V–T and vibration–vibration (V–V) reaction mechanisms. Of the three species (O_2, N_2, and O) considered for the air mixture, only the species N_2 was treated as an anharmonic oscillator with the following energy exchange mechanisms:

$$\dot{\omega}_v = (\rho_{N_2-N_2})^{V-T} + (\rho_{N_2-N_2})^{V-V} + (\rho_{N_2-O_2})^{V-T} + (\rho_{N_2-O})^{V-T} \tag{6}$$

The density of molecular nitrogen is the sum of population densities in the various vibrational levels:

$$\rho_{N_2} = \sum_{v=0,1,\ldots} \rho_v \tag{7}$$

The mass conservation of diatomic and atomic oxygen is represented by Eq. (2). The production of small amounts of atomic oxygen due to dissociation of diatomic oxygen is included in the source term $\dot{\omega}_s$. The mixture density ρ is the sum of the partial species densities,

$$\rho = \sum(\rho_{N_2} + \rho_{O_2} + \rho_O) \tag{8}$$

The conservation of total momentum is given by Eq. (3). Equation (4) is the conservation equation for vibrational energy. For diatomic nitrogen, a separate vibrational conservation equation was not necessary because the vibrational energy was calculated at each quantum level, discussed later. However, for the diatomic oxygen molecules assumed as harmonic oscillators, Eq. (4) was solved with a source term for the V–T coupling, modeled according to the Landau–Teller[8] (also see Ref. 9) form:

$$\dot{\omega}_{\text{vib}} = \left(e^*_{\text{vib}_s} - e_{\text{vib}_s}\right)\Big/\tau_s \tag{9}$$

where e_{vib_s} is the vibrational energy of the species O_2 and $e^*_{\text{vib}_s}$ is the vibrational energy in thermal equilibrium at the local translational temperature. The relaxation time is given by

$$\tau_s = \frac{\sum_s X_s}{\sum_s X_s/\tau_{\text{LT}}} \tag{10}$$

where X_s denotes the species mole fraction and τ_{LT} is the Landau–Teller interspecies relaxation times. Here τ_{LT} was computed using the expression developed by Millikan and White.[10] The vibrational temperature of O_2 was determined by inverting the expression for the vibrational energy contained in a harmonic oscillator at the temperature Tv,

$$e_{\text{vib}(O_2)} = \frac{R\Theta_{v(O_2)}}{e^{\Theta_{v(O_2)}/Tv} - 1} \tag{11}$$

where R is the species gas constant per unit mass. The V–V exchanges were neglected for the oxygen molecules in the present study. In a similar work, Candler and Kelley[7] neglected the V–V exchanges for all of the molecules where the relaxation time of V–T energy transfer of the N_2–O and O_2–O collisions is four orders of magnitude greater than that for highly nonresonant V–V energy exchanges between N_2 and O_2 at 1000 K (Ref. 11).

The kinetics of the particle exchanges among the quantum states of N_2 were simulated by the vibrational master equation. The population distributions were calculated by[6,12]

$$\dot{\omega}_v = \frac{1}{M}\left\{\sum_{v'}[k_{\text{VT}}(v' \to v)\rho_{v'}\rho - k_{\text{VT}}(v \to v')\rho_v\rho] + \sum_{w,v',w'}[k_{\text{VV}}(v', w' \to v, w)\rho_{v'}\rho_{w'} - k_{\text{VV}}(v, w \to v', w')\rho_v\rho_w]\right\} \tag{12}$$

where v' and w' are equal to $v - 1$ and $w - 1$, respectively. The equations governing the V–T reactions responsible for the variation of the particles distributed in the vth vibrational level of diatomic nitrogen are

$$N_2(v) + M \rightleftharpoons N_2(v-1) + M \tag{13}$$

where M represents O_2, O, and N_2. The equations governing the V–V processes in N_2 giving the reactions responsible for the variation of the particles distributed in the vth vibrational level are

$$N_2(v) + N_2(w) \rightleftharpoons N_2(v-1) + N_2(w-1) \tag{14}$$

For the kinetics of diatomic nitrogen, the present study used 1) V–T forward rate coefficients calculated according to expressions proposed by Capitelli et al.[13] and Billing and Fisher[14] and 2) V–V forward rates by Doroshenko et al.[15] The V–T forward rate coefficient for N_2–O collisions was from the work of Capitelli et al.,[16] which was based on Refs. 17 and 18. Backward rate coefficients were derived from detailed balance.

In the present study, for the N_2–O_2 collisions, the Landau–Teller theory was used to determine the V–T relaxation time[8] τ_{LT}, from Millikan and White correlations.[10] The rate constant $k_{1,0}$ for the (1,0) levels needed to obtain the reaction rates is

$$k_{1,0} = 1/\tau_{LT}[1 - \exp(-\Theta_v/T)] \tag{15}$$

The forward, $k_{v-1,v}$, and backward, $k_{v,v-1}$, rates were scaled from the rate constants $k_{1,0}$ (Ref. 9):

$$k_{v-1,v} = vk_{1,0}\exp(-\Theta_v/T) \tag{16}$$

$$k_{v,v-1} = vk_{1,0} \tag{17}$$

Although there is uncertainty in the reaction rate data used in the present study, the research was conducted with the intent of obtaining a qualitative understanding of the vibrational relaxation in air for hypersonic blunt body flows with $Tv > T$ behind the shock wave.

The vibrational energy of the N_2 molecule is given in terms of the quantum level energies by

$$e_{\text{vib}_{N_2}} = \frac{N_A}{M}\sum_{i=1,2,\ldots}\frac{\rho_i}{\rho_{N_2}}\epsilon_i \tag{18}$$

where i is used to denote the quantum level. In this equation, N_A is Avogadro's number, ρ_i/ρ_{N_2} is the fractional population of the ith vibrational level, M is the molecular weight, and ϵ_i the quantum level energy given by the third-order approximating formula

$$\epsilon_i/hc = \omega_e\left(i-\tfrac{1}{2}\right) - \omega_e x_e\left(i-\tfrac{1}{2}\right)^2 + \omega_e y_e\left(i-\tfrac{1}{2}\right)^3$$
$$i = 1, 2, \ldots, l \tag{19}$$

Equation (19) represents anharmonic-oscillator behavior of the N_2 molecule, where h is the Planck's constant, and c is the speed of light. The spectroscopic constants are given by[19] $\omega_e = 2358.57$ cm^{-1}, $\omega_e x_e = 14.324$ cm^{-1}, and $\omega_e y_e = -0.00226$ cm^{-1}. When $i = 45$, the value of energy exceeds the N_2 dissociation energy, 9.62 eV (Ref. 20). The present computations assume the number of vibrational quantum levels for the N_2 molecule as $i = 40$.

The first-level vibrational temperature T_{fl} defined as the temperature corresponding to the Boltzmann distribution of the population ρ_1/ρ_{N_2} of the first vibrational level is calculated by solving the equation

$$\frac{\rho_1}{\rho_{N_2}} = \exp\left(\frac{-\epsilon_1}{kT_{fl}}\right)\Big/\sum_{j=1,2,\ldots}\exp\left(\frac{-\epsilon_j}{kT_{fl}}\right) \tag{20}$$

where k is the Boltzmann constant. In the present study, T_{fl} is used to represent the vibrational temperature of the anharmonic N_2 molecule. Note that T_{fl} is not very indicative of a vibrational temperature in the case of highly non-Boltzmann distributions.

The V–T forward relaxation times for the N_2–O_2, N_2–N_2, and the N_2–O reactions are plotted at various temperatures in Fig. 1. It is clearly seen that the times for the N_2–O_2 and N_2–N_2 collisions are nearly the same for the entire range of temperatures (also noted in Ref. 21); the relaxation times for N_2–O collisions, in comparison, are significantly less. The faster rates of the N_2–O collisions contribute to V–T energy losses, altering the kinetics of reactions behind the shock wave. The experimental measurements in the temperature range of 3000–4000 K are about an order of magnitude lower than the analytical results, confirming the large discrepancy in relaxation time between the molecule–molecule and N_2–O collisions. See Table 1 for a summary of the rates used for the different

Table 1 Details of rates used for vibrational energy transfer

No.	Species	Type oscillator	Collides with	V–T rates from	V–V rates from
1	N_2	Anharmonic	N_2	Ref. 13	Ref. 15
2	N_2	Anharmonic	O_2	Ref. 10	——
3	N_2	Anharmonic	O	Ref. 16	——
4	O_2	Harmonic	N_2, O	Ref. 10	——

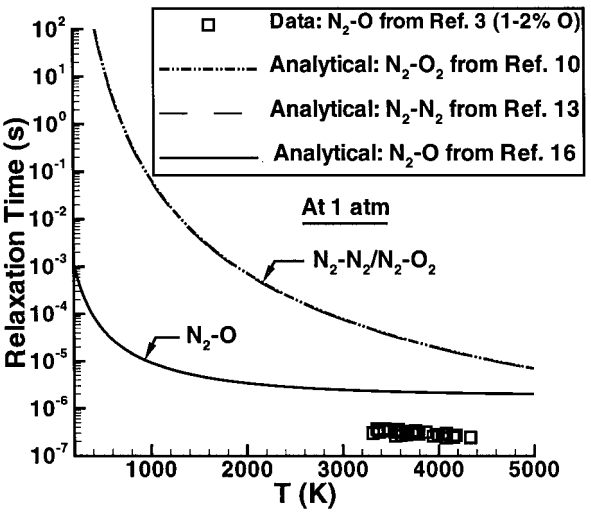

Fig. 1 V–T forward relaxation times at 1 atm.

cases computed in the present study. The primary species of air considered in the present study were O_2, O, and N_2. For the maximum shock temperature of 3000 K, the significant chemical reactions between the species considered are

$$O_2 + M \rightleftharpoons 2O + M \tag{21}$$

The chemical source terms are derived from the law of mass action. The reaction rates and equilibrium constants were taken from the work of Park.[22] The vibration–dissociation coupling for the diatomic species was achieved by the two-temperature model suggested by Park[22]: $T_f = \sqrt{(TT_v)}$, where T_f is the rate-controlling temperature for the forward rate of the dissociation–recombination reactions. The freestream air mixture for the Mach 6.5 flow consisted of 0.0001% O atoms. For this case, the shock temperature of nearly 3000 K produced minor amounts of oxygen atoms in the shock layer by O_2 dissociation, which allowed us to study effects of atomic oxygen on N_2 relaxation. In the case of Mach 1.5 flow, however, there is no oxygen dissociation for the low shock temperatures (less than 500 K); hence, the present study considered two mixtures of freestream air, which included 1) 0.1% O and 2) 1% O. The inclusion of the additional oxygen atoms was necessary for this case to study the effect of the N_2–O collisions on the V–T energy loss in the flowfield.

Conditions of Numerical Simulation

Several cases were run to validate the present code and to study the physics of nonequilibrium flow past a blunt body. A Mach 6.5 flow past a 1-m-radius infinite cylinder was computed for two types of media, pure nitrogen and air mixtures, to compare results with an existing computation[23] and to quantify variation of the results in air from those of pure nitrogen. Experimental shock-standoff distances available[24] for Mach 7.7 and 8.6 airflows past smaller radii spheres, 0.014 and 0.015 m, respectively, were computed to enable validation of the present code. As part of code validation, the present air code compared results of N_2 assumed as an anharmonic and a harmonic oscillator; O_2 was treated as a harmonic oscillator in both calculations.

The effect of the oxygen atoms on N_2 relaxation was studied for flow at Mach 6.5 and at a lower Mach number of 1.5 past a

Table 2 Details of flow conditions in freestream

Case	Mach no.	T_∞, K	Tv_∞, K	p_∞, Pa	Radius r, m	Medium	Validation
1[a]	6.5	300	300	50	1.0	N_2, air (0.0001% O)	Comparison with Ref. 23
2	7.7	293	293	600	0.014	Air (0.0001% O)	Experiment/comparison with Ref. 24
3	8.6	293	293	560	0.015	Air (0.0001% O)	Experiment/comparison with Ref. 24
4	6.5	300	4000	50	1.0	N_2, air (0.0001% O)	——
5	1.5	300	4000	50	1.0	N_2, air (0.1% O)	——
6	1.5	300	4000	50	1.0	N_2, air (1% O)	——

[a]Case 1 is two-dimensional infinite cylinder, all other cases are hemisphere cylinders.

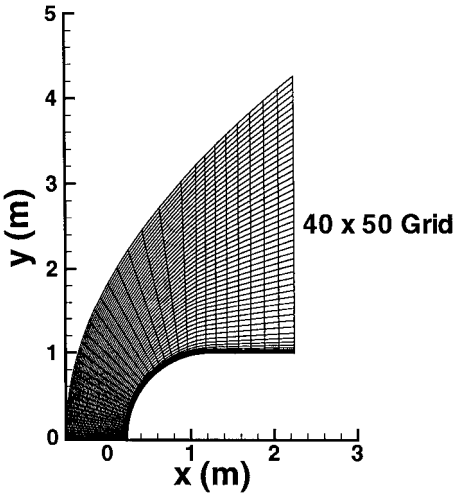

Fig. 2 Typical computational grid.

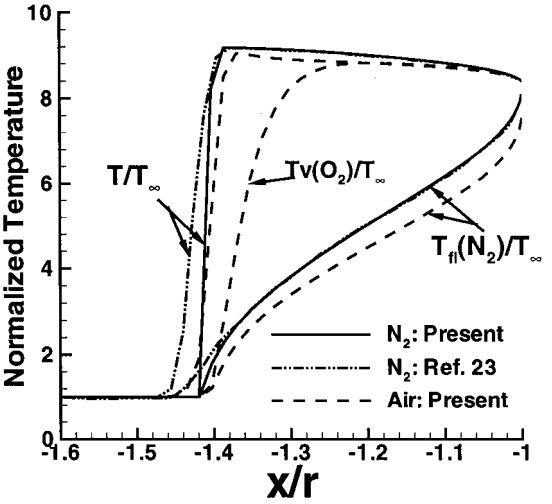

Fig. 3 Validation: comparison of temperatures along stagnation streamline, $M_\infty = 6.5$, $p_\infty = 50$ Pa, $Tv_\infty = 300$ K, $T_\infty = 300$ K, and $r = 1$ m.

hemisphere cylinder. At both Mach numbers, the freestream conditions were in nonequilibrium to produce $Tv > T$ behind the shock. The lower Mach number selected for the purpose of delineating the effects of V–T losses consisted of cases where the air mixtures had varying amounts of oxygen atoms, 0.0001, 0.1, and 1%. A summary of these cases is given in Table 2.

The numerical algorithm used to solve the coupled set of equations is the Roe flux difference method with an entropy correction used in Ref. 6. An explicit predictor–corrector method is used to advance the solution in time.

A grid-size study was conducted to determine the effects of grid density on the temperature distribution along the stagnation streamline and surface. Details are given in Ref. 6. A mesh system of 40 nodes in the body-tangential direction and 50 nodes in the body-normal direction was used for all of the cases in the present study. The grid system for the two-dimensional cylinder is shown in Fig. 2. The minimum distance Δ_n/r of the first mesh point away from the body was 0.0012, and the grid was exponentially stretched in the body-normal direction with a stretch factor of 1.27.

Convergence to a steady-state solution was monitored by the L_2 norm. The data processing rate (DPR) of the pure nitrogen code for the two-dimensional solution of the Euler equations using the vibrational kinetics model with 40 quantum levels is 7.5×10^{-4} CPU-s/point/iteration on a single processor of a Cray C-90 computer.

Boundary Conditions

The upstream and farfield boundary conditions were prescribed as the undisturbed freestream values. At the downstream boundary, the no-change condition was imposed for the predominantly supersonic flowfield. On the body surface, $\boldsymbol{n} \cdot \boldsymbol{u}$ is zero, where $\boldsymbol{n}$ is the surface normal vector. The finite volume formulation of the present work allows fluxes at the singular line of symmetry to be set to zero because the control surface of the elementary cell at the axis of symmetry merges to a point.

The population densities in N_2 were set to values corresponding to a Boltzmann distribution at the temperature Tv_∞ on the first i levels of the spectrum produced by Eq. (19). Thus, $\rho_{i,\infty}$ is given by

$$\frac{\rho_{i,\infty}}{\rho_{N_2\infty}} = \exp\left(\frac{-\epsilon_i}{kTv}\right) \Bigg/ \sum_{j=1,2,\ldots} \exp\left(\frac{-\epsilon_j}{kTv}\right) \qquad i = 1, \ldots, l \qquad (22)$$

where k is the Boltzmann constant. Vibrational temperature Tv in the freestream is either in equilibrium with translational temperature producing vibrational heating in the shock layer or in nonequilibrium with T producing vibrational cooling in the shock layer.[6] Tv for O_2 and N_2 molecules was set to the same value in the freestream. See Table 2 for a summary of flow conditions used in the present study. Initial conditions were set to freestream uniform flow conditions.

Results and Discussion

Results are discussed in two sections. Comparison of the present computations with experimental data and previously reported computations to validate the code comprise the first section. The second section shows effects of minor amounts of oxygen atoms on air mixtures flowing past a hemisphere cylinder where $Tv > T$ behind the shock wave.

Population distributions vs quantum level vibrational energies [Eq. (19)] are plotted on select locations along the stagnation streamline. The locations are preshock, postshock, in shock layer, and stagnation point. The preshock location (at the shock edge) is at the grid point immediately before the jump in T and p to their highest value across the shock, and the postshock location is the point immediately behind the shock front in the shock layer.

Validation

Figure 3 shows comparisons of temperature distribution in the flowfield for $M_\infty = 6.5$, $p_\infty = 50$ Pa, and $T_\infty = 300$ K, for pure

nitrogen and airflow past an infinite cylinder of 1-m radius. Figure 3 shows comparison along stagnation streamline with existing computation[23] in pure nitrogen. The comparison of results in pure nitrogen shows that the translational and first-level vibrational temperatures along the stagnation streamline are in good agreement. The slight discrepancy of the translational temperature jump across the shock between the present and Ref. 23 results is due to difference in grid sizes and algorithms used for the respective computations. For the present computation in air (also shown in Fig. 3), the vibrational temperature of O_2 goes up across the shock and equilibrates with the translational temperature in the shock layer. The energy associated with raising the vibrational temperature of O_2, brings the postshock location toward the body with a lower translational temperature throughout the shock layer. The lowering of the translational temperature of air in the shock layer and recovery at the stagnation region are due to the overfilling of the high vibrational states and the subsequent relaxation, reducing the vibrational population in the higher states. The lower translational temperature in the air mixture has a lower $T_{fl}(N_2)$ compared to that of pure nitrogen (Fig. 3)

For validating the present code with experimental data,[24] comparisons of shock-standoff distance and temperature distributions along the stagnation streamline were made in Figs. 4a and 4b, respectively. The two cases computed were for Mach 7.7 and 8.6 airflow past hemisphere cylinders (see Table 2 for details on flow conditions). The comparison of shock-standoff distance at the two freestream velocities is shown in Fig. 4a. The reference frozen flow curve (taken from Ref. 25) shows that both cases have a small departure from chemically frozen conditions. The comparison shows that computations at both velocities are within 1% of each other. The shock-standoff distance prediction is 1% higher than data for the Mach 7.7 case and 3% lower than data for the Mach 8.6 case. The temperature distributions along the stagnation streamline for these cases are shown in Fig. 4b. The comparison between the present Euler computation and the Ref. 24 viscous computation is remarkably good throughout the shock layer; across the shock wave the difference, as noted earlier, is within 1%.

The population distribution in Fig. 4c shows a higher fractional state density of N_2 for the higher velocity case, and as expected, the population distribution at the stagnation point is close to Boltzmann distribution.

It can be concluded that the present air code using vibrational kinetic formulation for N_2 molecules predicts with good accuracy the shock-standoff distance in intermediate hypersonic flows.

Effects of Atomic O on N_2 Relaxation

Results are now shown for a Mach 6.5 flow past a hemisphere cylinder of 1 m radius. The flow media considered are pure nitrogen and an air mixture with 0.0001% O in the freestream. Comparisons of temperatures along the stagnation streamline are shown in Fig. 5, the mass fraction of atomic oxygen (along the stagnation streamline) produced by the O_2 dissociation in Fig. 6, and comparisons of temperatures along the surface in Fig. 7. The freestream conditions of this flow are such that the vibrational temperatures of oxygen and nitrogen are about 13 times the translational temperature of 300 K. This results in $Tv > T$ behind the shock, and the vibrational modes undergo cooling in the shock layer (Ref. 6 for more discussion on the physics of the vibrational cooling flows). The translational temperature T along the stagnation streamline in Fig. 5 jumps up by about nine times its freestream value. T increases in the shock layer, with the energy transfer by V–T mechanism lowering the vibrational temperature, reaching near equilibrium conditions at the stagnation point. Figure 5 shows that the air mixture reaches thermal equilibrium at the stagnation point. The vibrational temperature of O_2, however, equilibrates with the translational temperature in the shock layer before the flow reaches the stagnation point. As the flow enters the stagnation region, the atomic oxygen concentration increases to 0.1% due to the dissociation of O_2 (Fig. 6), thus increasing the rapid N_2–O collisions that enhance the N_2 relaxation. This lowers the $T_{fl}(N_2)$ in air compared to pure nitrogen in the stagnation region shown in Fig. 5. The high vibrational temperature of O_2 specified in the freestream introduces additional energy of vibration in the air

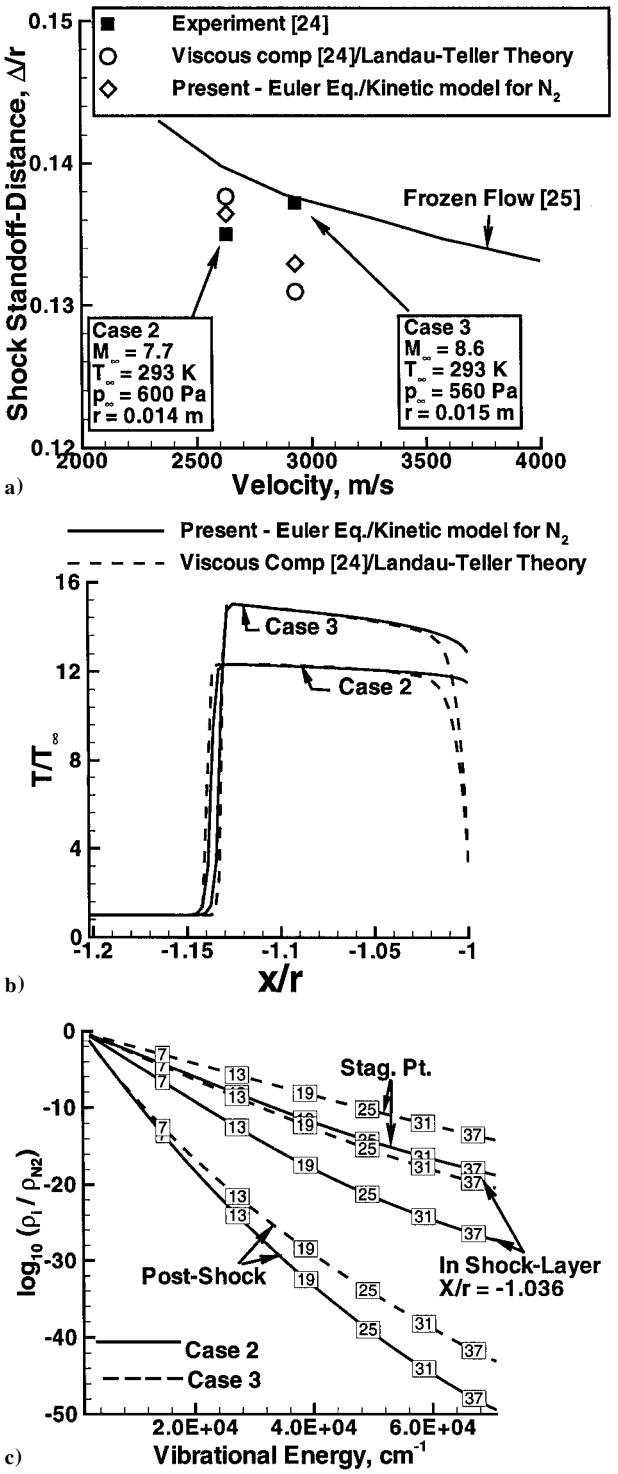

Fig. 4 Validation: comparison of a) shock-standoff distance with experimental data, b) translational temperature with existing computation along stagnation streamline, and c) population distribution along stagnation streamline.

mixture causing greater shock-standoff distance (see Fig. 5 and its inset).

The surface temperatures in Fig. 7 show the first level vibrational temperature of N_2 nearly constant along the forebody; the $T_{fl}(N_2)$ of the air mixture is lower than that of pure nitrogen by about 5%. The translational temperatures of pure nitrogen and the air mixture reduce from the stagnation point to the shoulder, the expansion cooling the flow. The population distribution of N_2 (Fig. 8) at the postshock and stagnation point locations are vibrationally cooled and are close to Boltzmann distribution. The fractional state densities of N_2 in the air mixture are less than those of pure nitrogen at

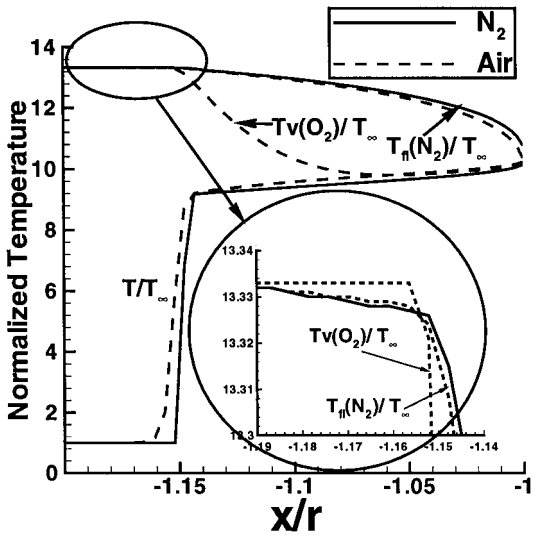

Fig. 5 Temperature along stagnation streamline, $M_\infty = 6.5$, $p_\infty = 50$ Pa, $Tv_\infty = 4000$ K, $T_\infty = 300$ K, and $r = 1$ m.

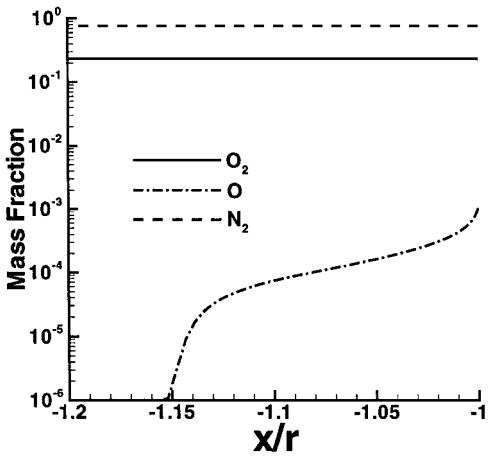

Fig. 6 Species mass fraction distribution along stagnation streamline for air mixture (O in freestream = 0.0001%), $M_\infty = 6.5$, $p_\infty = 50$ Pa, $Tv_\infty = 4000$ K, $T_\infty = 300$ K, and $r = 1$ m.

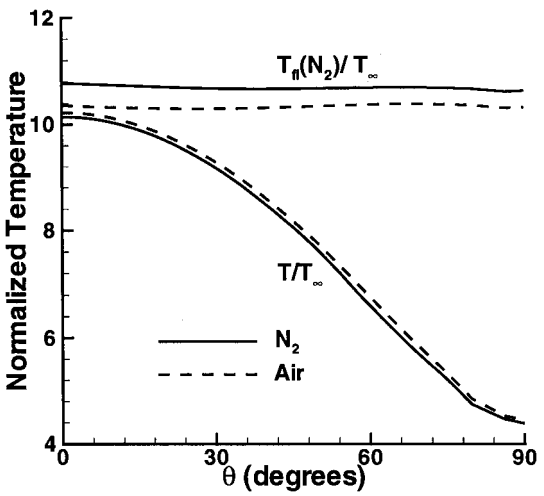

Fig. 7 Temperature distribution along surface, $M_\infty = 6.5$, $p_\infty = 50$ Pa, $Tv_\infty = 4000$ K, $T_\infty = 300$ K, and $r = 1$ m.

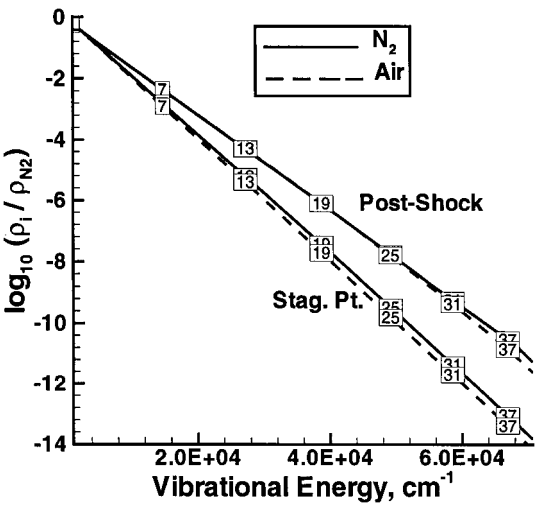

Fig. 8 Population distribution along stagnation streamline, $M_\infty = 6.5$, $p_\infty = 50$ Pa, $Tv_\infty = 4000$ K, $T_\infty = 300$ K, and $r = 1$ m.

the stagnation point, a result of greater vibrational relaxation of N_2 in the presence of oxygen atoms.

The effect of oxygen atoms on the airflow past a hemisphere cylinder at a lower Mach number of 1.5 is now discussed. The conditions of simulation are such that the translational temperatures are less than 450 K, at which the V–T energy loss is more significant than V–V exchanges. At these temperatures, O_2 dissociation is absent. To study the effect of oxygen atoms on N_2 relaxation in the air mixture, varying amounts of oxygen atoms were introduced in the flowfield. The nonequilibrium freestream conditions for this flow are $T_\infty = 300$ K, $Tv_\infty = 4000$ K, $p_\infty = 50$ Pa, and the hemisphere radius is 1 m. Figure 9 shows the translational and vibrational temperatures along the stagnation streamline for the following freestream media: 1) pure nitrogen, 2) air with 0.1% O, and 3) air with 1% O. From the translational temperature comparison, it is seen that the shock-standoff distance increases with increase in percentage of oxygen atoms. The shock-standoff distance in the air mixture with 0.1% O increases by 4% over that of N_2; the increase in air mixture with 1% O is about 3% more than with 0.1% O. This is a result of V–T energy transfer of the N_2–O collisions, which, discussed for Fig. 1, is about two orders more efficient than either the N_2–N_2 or N_2–O_2 collisions. Also, the translational temperature increases in the shock layer as the flow approaches the body, with an increase in the oxygen atom concentration. At the stagnation point, the translational temperature decreases for the pure nitrogen and the air mixture with 0.1% O due to the slower V–T rates of N_2–N_2 and N_2–O_2 at the lower temperatures; however, with an increase in percentage of oxygen atoms to 1%, the effect of the N_2–O collision rate is to increase the translational temperature. The V–T heating rate in the quantum energy states of N_2 in air of varying oxygen atom concentrations is discussed later. The nonlinearity of the temperature profiles near the surface is dependent on the accuracy of the V–T reaction rates at the low temperatures.

It may be concluded from results shown in Figs. 5 and 9 that the mass fraction of the oxygen atoms above 0.1% begins to control the V–T rates.

The first-level vibrational temperature of N_2 in Fig. 9 shows a corresponding decrease in the freestream and a larger decrease in the shock layer, undergoing vibrational cooling. Interestingly, the $T_{fl}(N_2)$ of the air mixture with 0.1% O is higher than that of the pure nitrogen medium. This is due to the reduction of population in the high vibrational states driving the population up in the lower states and making the $T_{fl}(N_2)$ higher for the air mixture. Note the crossover of the population distribution at $i = 5$ of N_2 in the air mixture with 0.1% O, shown later. As the atomic oxygen is increased to 1%, the population is depleted in the higher as well as lower states due to quenching. This reduces the $T_{fl}(N_2)$ for air with 1% O compared to pure nitrogen in the postshock and stagnation regions. In the rest of the shock layer, $T_{fl}(N_2)$ of the air mixture with 1% O has about

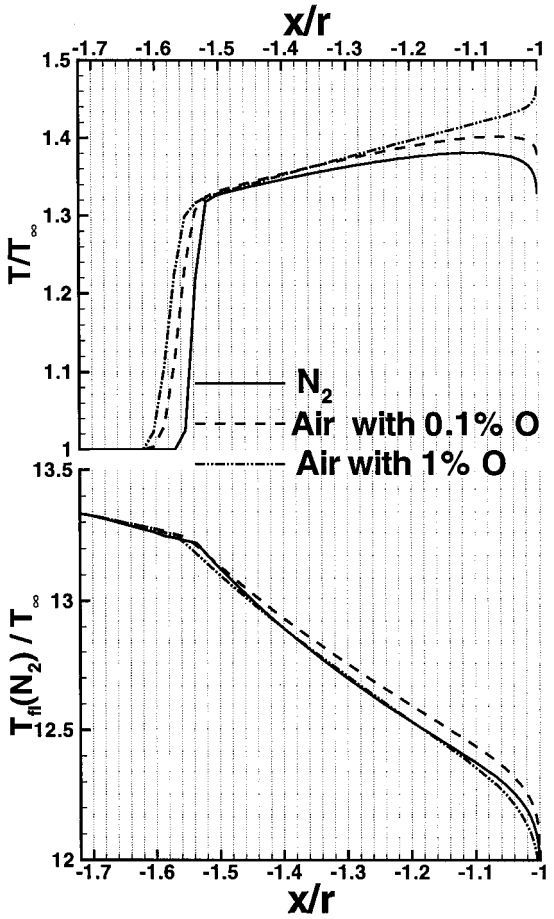

Fig. 9 Temperature distribution along stagnation streamline, $M_\infty = 1.5$, $p_\infty = 50$ Pa, $Tv_\infty = 4000$ K, $T_\infty = 300$ K, and $r = 1$ m.

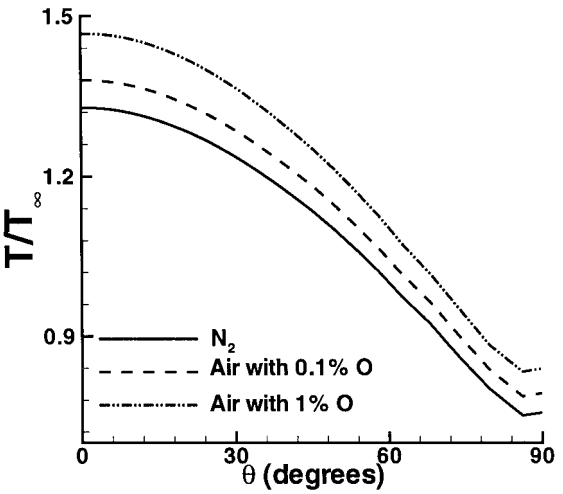

Fig. 10 Translational temperature along surface, $M_\infty = 1.5$, $p_\infty = 50$ Pa, $Tv_\infty = 4000$ K, $T_\infty = 300$ K, and $r = 1$ m.

the same temperature as in the pure nitrogen medium because the depletion of the vibrational population in the higher levels increases the population in the lower levels, which are quenched due to the N_2–O collisions.

The translational temperature distribution along the surface for the pure nitrogen and air mixtures is shown in Fig. 10. The temperatures increase with increase in percentage of oxygen, as expected. An increase of 4% for air (0.1% O) over the pure nitrogen medium and an increase of 6.5% for air (1% O) over air (0.1% O) is achieved. The drop in the translational temperature from the stagnation point to the shoulder along the forebody is due to the expansion of the flow.

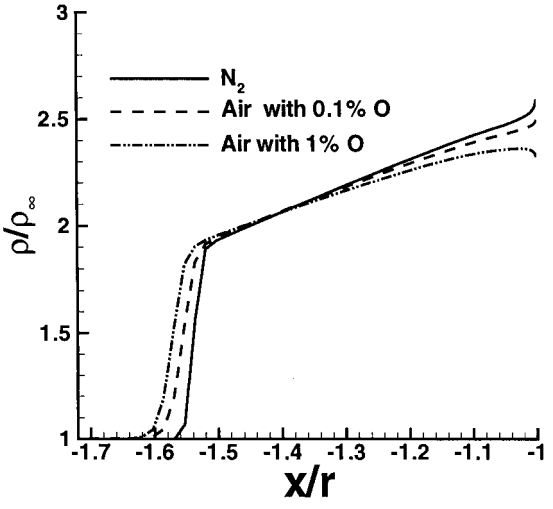

Fig. 11 Density distribution along stagnation streamline, $M_\infty = 1.5$, $p_\infty = 50$ Pa, $Tv_\infty = 4000$ K, $T_\infty = 300$ K, and $r = 1$ m.

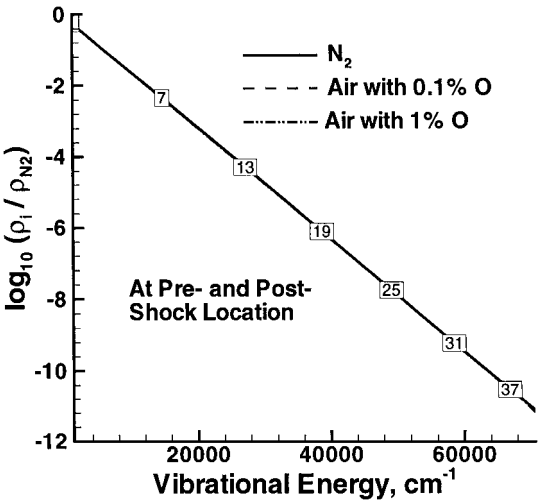

Fig. 12 Population distribution at pre- and postshock location of stagnation streamline, $M_\infty = 1.5$, $p_\infty = 50$ Pa, $Tv_\infty = 4000$ K, $T_\infty = 300$ K, and $r = 1$ m.

The mixture density variation along the stagnation streamline (Fig. 11) shows the increase in shock-standoff distance for the air mixtures with increasing oxygen concentrations and a decrease in the shock layer from $X/r = -1.3$ to the stagnation point $(X/r = -1)$.

The population distributions in the N_2 vibrational states in the pre/postshock, in the shock layer, and at the stagnation point are shown in Figs. 12–14. The population distribution in the preshock location of stagnation streamline (Fig. 12) for the pure nitrogen and air mixtures is nearly the same and is Boltzmann distribution. The distribution behind the shock wave (Fig. 13a) is shown at the postshock location and at a distance of 0.13 m from the body along the stagnation streamline. The distribution is Boltzmann in the immediate postshock location of the shock wave; at a distance 0.13 m from the body, the distribution is non-Boltzmann by the V–V up pumping between the levels of 9 and 25 and the V–T losses in the upper levels. In the shock layer, the air with 1% O has the lowest fractional state density in the upper levels of N_2 (shown in Fig. 13b), air with 0.1% O has higher, and pure nitrogen the highest. In the shock-layer location, the V–T energy losses in the upper levels are higher for air with the higher oxygen concentration due to the N_2–O collisions. As noted earlier in the discussion of Fig. 9, for the air mixture with 0.1% O atoms, the reduction of population in the upper levels drives the population up in the lower levels as seen by the crossover in Fig. 13c. For the higher oxygen fraction of 1%, quenching occurs in all of the vibrational states, thus reducing the population distribution throughout.

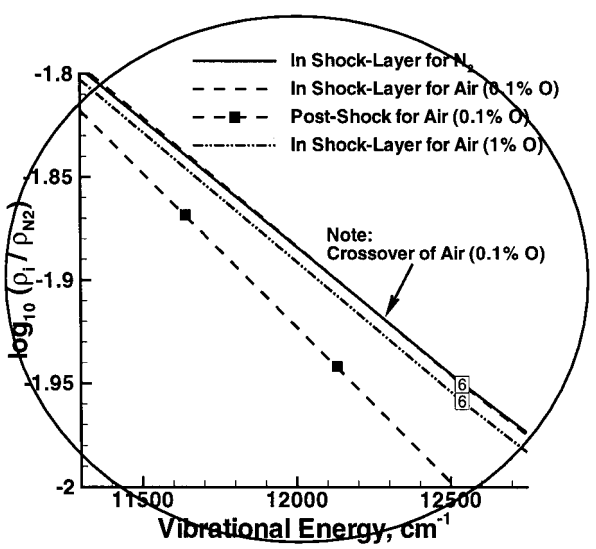

b) Blowup at lower vibrational levels

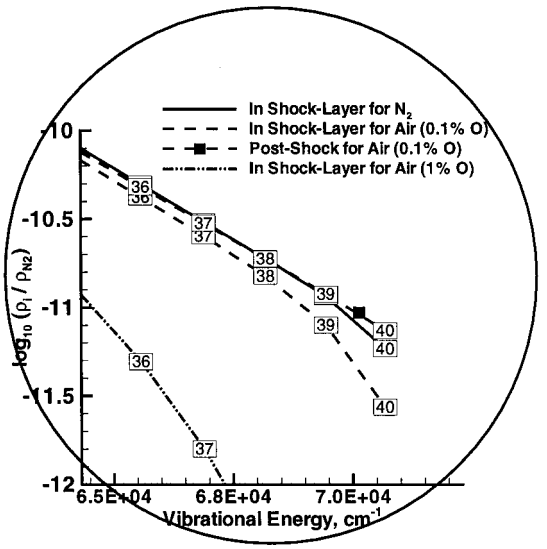

c) Blowup at upper vibrational levels

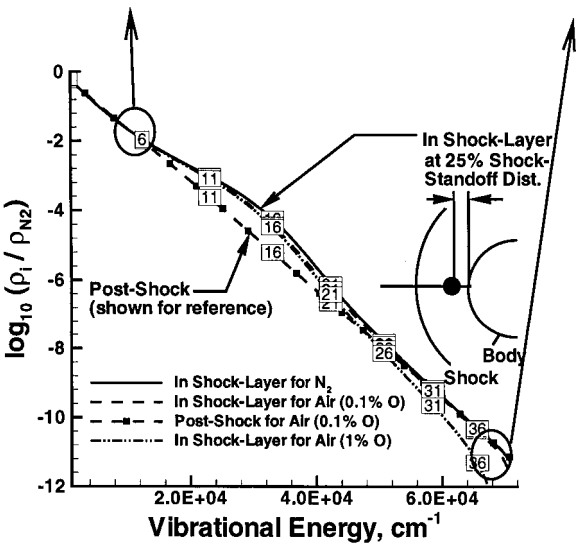

a) Along stagnation streamline at post-shock and in shock layer at 0.13 m from body

Fig. 13 Population distribution, $M_\infty = 1.5$, $p_\infty = 50$ Pa, $Tv_\infty = 4000$ K, $T_\infty = 300$ K, and $r = 1$ m.

At the stagnation point (shown in Fig. 14), there is even greater non-Boltzmann behavior associated with V–V and V–T transfers. The fractional state density is lowest for high vibrational states of N_2 in air with higher oxygen concentrations. Figures 13 and 14 do not, however, give an indication of which vibrational levels are responsible for the V–T heating rates affecting the temperatures shown in Fig. 9. The V–T heating rates in the vibrational energy levels of N_2 are shown for the postshock and stagnation point locations in Fig. 15.

The V–T heating rate R_{VT} due to the N_2–O collision is given by the difference in the vibrational excitation and relaxation rates as

$$R_{VT} = \sum_{v=0,1,\ldots} \left(\rho_{v_{N_2}} \rho_O F^{VT}_{v,v-1} - \rho_{v-1_{N_2}} \rho_O B^{VT}_{v-1,v}\right)(\epsilon_v - \epsilon_{v-1}) \quad (23)$$

where F and B are the forward and backward reaction rates, respectively, ϵ is the quantum level vibrational energy, $\rho_{v_{N_2}}$ is the population density in the vth vibrational level of N_2, and ρ_O is the density of atomic oxygen. The equation provides a quantitative comparison of the vibrational levels that contribute toward the heating due to V–T energy transfers. R_{VT} plotted in Fig. 15 shows the rate in air

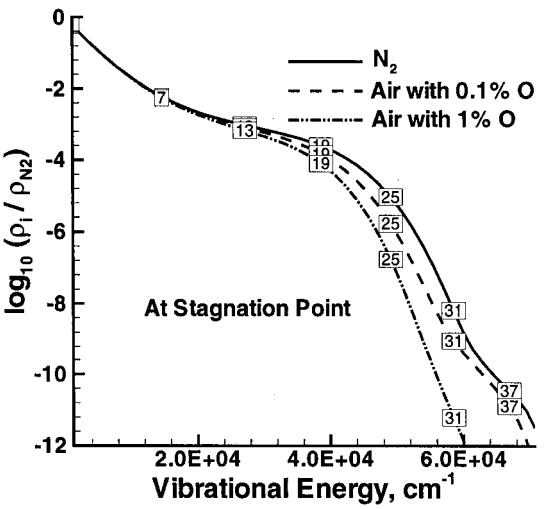

Fig. 14 Population distribution at stagnation point, $M_\infty = 1.5$, $p_\infty = 50$ Pa, $Tv_\infty = 4000$ K, $T_\infty = 300$ K, and $r = 1$ m.

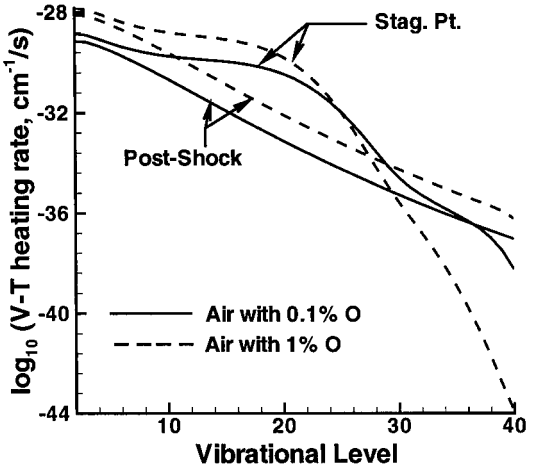

Fig. 15 Heating rate due to V–T transfers, $M_\infty = 1.5$, $p_\infty = 50$ Pa, $Tv_\infty = 4000$ K, $T_\infty = 300$ K, and $r = 1$ m.

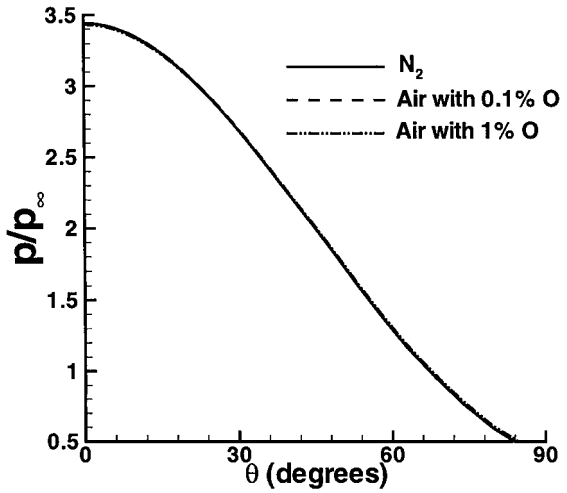

Fig. 16 Surface pressure distribution, $M_\infty = 1.5$, $p_\infty = 50$ Pa, $Tv_\infty = 4000$ K, $T_\infty = 300$ K, and $r = 1$ m.

with concentrations of 0.1 and 1% O. As expected, the medium with greater concentration of oxygen atoms has a greater heating rate due to the high efficiency of the N_2–O collisions. At both atomic oxygen concentrations, the lower vibrational levels make a greater contribution to heating, and for the flow at the stagnation point, the upper levels from 10 to 20 also make a significant contribution to heating.

The surface pressure on the forebody (Fig. 16) remains the same for the Mach 1.5 airflow with varying amounts of oxygen concentrations.

Concluding Remarks

A computational study of hypersonic airflow past a hemisphere cylinder was conducted. The flow conditions were Mach number 6.5 at $p_\infty = 50$ Pa and $T_\infty = 300$ K and $Tv_\infty = 4000$ K for a 1-m-radius body. A Mach 1.5 flow was also computed to isolate effects of the V–T heating resulting from N_2–O collisions. The inviscid Euler equations were coupled to the vibrational master equations with 40 quantum energy levels of diatomic nitrogen, assumed as an anharmonic oscillator. The master equations account for the V–T and V–V energy exchange processes. The flow media considered were pure nitrogen and air mixtures of atomic oxygen concentrations of 0.0001, 0.1, and 1%.

Comparisons of the present results with a previously reported computation show excellent agreement in the predictions of translational temperatures and first-level vibrational temperatures along the stagnation streamline. Comparison of shock-standoff distance with experimental data agreed favorably.

For the Mach 6.5 flow past a 1-m-radius hemisphere cylinder, the freestream air mixture consisting of 0.0001% O has a mass fraction of 0.1% O near the body due to the O_2 dissociation; the presence of these oxygen atoms decreases the translational temperature in air compared to pure nitrogen near the body. For the Mach 1.5 flow, O_2 dissociation is absent; hence, the freestream air mixture was specified as having of 0.1 and 1% O atoms, in the present study. The air mixture with 0.1% and higher oxygen concentrations causes heating in the shock layer, which increases the translational temperature in the shock layer and increases the shock-standoff distance. The increases in the shock-standoff distances are accompanied by the lowering of densities in the shock layer. The maximum V–T heating rate in the shock layer occurs in the lower five levels, with the heating rate increasing in higher levels (up to 20) as the flow approaches the body. The effect of high V–T energy losses at the higher quantum numbers lowers the fractional state density beyond quantum number of 25 away from the Boltzmann distribution. V–T losses in the higher vibrational states for the air mixture with 0.1% oxygen atoms drive up the vibrational population in the lower states, which increases the vibrational temperature from that of pure nitrogen, but an increase to 1% atomic oxygen quenches the vibrational population in all of the vibrational states and lowers the vibrational temperature from that of pure nitrogen. Near the surface, the rate-controlling oxygen mass fraction in the air mixture for the N_2–O collisions to be effective is noted as 0.1%. The surface pressure for the Mach 1.5 flow with varying amounts of oxygen concentrations shows no variation.

Acknowledgments

This research was supported under Air Force Office of Scientific Research contracts monitored by R. Canfield and S. Walker. A major part of the computer resources was provided by the Department of Defense High Performance Computing Major Shared Resource Center at the Naval Oceanographic Office, Bay St. Louis, Mississippi. The author is indebted to W. F. Bailey, Air Force Institute of Technology, for many helpful discussions.

References

[1]Treanor, P. V., Rich, J. W., and Rehm, R. G., "Vibrational Relaxation of Anharmonic Oscillators with Exchange-Dominated Collisions," *Journal of Chemical Physics*, Vol. 48, No. 4, 1968, pp. 1798–1807.

[2]Mishin, G. I., Bedin, A. P., Yushchenkova, G. E., and Ryazin, A. P., "Anomalous Relaxation and Instability of Shock Waves in Gases," *Soviet Physics—Technical Physics*, Vol. 26, No. 11, 1981, pp. 1363–1368.

[3]Breshears, W. D., and Bird, P. F., "Effect of Oxygen Atoms on the Vibrational Relaxation of Nitrogen," *Journal of Chemical Physics*, Vol. 48, No. 10, 1968, pp. 4768–4773.

[4]Center, R. E., "Vibrational Relaxation of CO by O Atoms," *Journal of Chemical Physics*, Vol. 58, No. 12, 1973, pp. 5230–5236.

[5]Zel'dovich, Y. B., and Raizer, Y. P., *Physics of Shock Waves and High Temperature Hydrodynamic Phenomena*, Academic, New York, 1966, pp. 356–362.

[6]Josyula, E., "Computational Study of Vibrationally Relaxing Gas past Blunt Body in Hypersonic Flows," *Journal of Thermophysics and Heat Transfer*, Vol. 14, No. 1, 2000, pp. 18–26.

[7]Candler, G. V., and Kelley, J. D., "Effect of Internal Energy Excitation on Supersonic Air Flow," AIAA Paper 99-4964, Nov. 1999.

[8]Landau, L., and Teller, E., "Zur Theorie der Schalldispersion," *Physikalische Zeitschrift der Sowjetunion*, Vol. 10, No. 1, 1936, pp. 34–43.

[9]Vincenti, W. G., and Kruger, C. H., Jr., *Introduction to Physical Gas Dynamics*, Wiley, New York, 1967, pp. 198–206.

[10]Millikan, R. C., and White, D. R., "Systematics of Vibrational Relaxation," *Journal of Chemical Physics*, Vol. 39, No. 12, 1963, pp. 3209–3213.

[11]White, D. R., and Millikan, R. C., "Vibrational Relaxation in Air," *AIAA Journal*, Vol. 2, No. 10, 1964, pp. 1844, 1845.

[12]Adamovich, I. V., Macheret, S. O., Rich, J. W., and Treanor, C. E., "Vibrational Relaxation and Dissociation Behind Shock Waves Part 2: Master Equation Modeling," *AIAA Journal*, Vol. 33, No. 6, 1995, pp. 1070–1075.

[13]Capitelli, M., Gorse, C., and Billing, G. D., "V–V Pumping Up in Nonequilibrium Nitrogen: Effects on the Dissociation Rate," *Chemical Physics*, Vol. 52, No. 3, 1980, pp. 299–304.

[14]Billing, G. D., and Fisher, E. R., "VV and VT Rate Coefficients in Diatomic Nitrogen by a Quantum Classical Model," *Chemical Physics*, Vol. 43, No. 3, 1979, pp. 395–401.

[15]Doroshenko, V. M., Kudryavtsev, N. N., Novikov, S. S., and Smetanin, V. V., "Effect of the Formation of Vibrationally Excited Nitrogen Molecules in Atomic Recombination in a Boundary Layer on the Heat Transfer," *High Temperature (USSR)*, Vol. 28, No. 1, 1990, pp. 82–89.

[16]Capitelli, M., Armenise, I., and Gorse, C., "State-to-State Approach in the Kinetics of Air Components Under Re-Entry Conditions," *Journal of Thermophysics and Heat Transfer*, Vol. 11, No. 4, 1997, pp. 570–578.

[17]Billing, G. D., "VV and VT Rates in N_2–O_2 Collisions," *Chemical Physics*, Vol. 179, No. 3, 1994, pp. 463–467.

[18]Mnatsakanyan, A. K., and Naidis, G. V., "The Vibrational-Energy Balance in a Discharge in Air," *High Temperature (USSR)*, Vol. 4, No. 3, 1985, pp. 506–513.

[19]Huber, K. P., and Herzberg, G., *Constants of Diatomic Molecules*, Van Nostrand Reinhold, New York, 1979, pp. 420–421.

[20]Armenise, I., Capitelli, M., Celiberto, R., Colonna, G., and Gorse, C., "The Effect of $N + N_2$ Collisions on the Non-equilibrium Vibrational Distributions of Nitrogen Under Reentry Conditions," *Chemical Physics Letters*, Vol. 227, No. 1, 1994, pp. 157–163.

[21]Wood, A. D., "Summary of Vibrational Energy Exchange Probabilities and Relaxation Times for Mixtures of CO_2, N_2, H_2O, He," TR TM-185, Avco Everett Research Lab., Everett, MA, March 1969.

[22]Park, C., "On Convergence of Computation of Chemically Reacting Flows," AIAA Paper 85-0247, Jan. 1985.

[23]Giordano, D., Bellucci, V., Colonna, G., Capitelli, M., Armenise, I., and Bruno, C., "Vibrationally Relaxing Flow of N_2 past an Infinite Cylinder," *Journal of Thermophysics and Heat Transfer*, Vol. 11, No. 1, 1997, pp. 27–35.

[24]Furudate, M., Nonaka, S., and Sawada, K., "Behavior of Two-Temperature Model in Intermediate Hypersonic Regime," *Journal of Thermophysics and Heat Transfer*, Vol. 13, No. 4, 1999, pp. 424–430.

[25]Lobb, R. K., "Experimental Measurement of Shock Detachment Distance on Sphere Fired in Air at Hypervelocities," *The High Temperature Aspects of Hypersonic Flow*, edited by W. C. Nelson, Pergamon, New York, 1964, pp. 519–527.